Prostate apoptosis response-4 mediates TGF-β-induced epithelial-to-mesenchymal transition

P Chaudhry[1,2], F Fabi[1,2], M Singh[1], S Parent[1], V Leblanc[1] and E Asselin*,[1]

A growing body of evidence supports that the epithelial-to-mesenchymal transition (EMT), which occurs during cancer development and progression, has a crucial role in metastasis by enhancing the motility of tumor cells. Transforming growth factor-β (TGF-β) is known to induce EMT in a number of cancer cell types; however, the mechanism underlying this transition process is not fully understood. In this study we have demonstrated that TGF-β upregulates the expression of tumor suppressor protein Par-4 (prostate apoptosis response-4) concomitant with the induction of EMT. Mechanistic investigations revealed that exogenous treatment with each TGF-β isoform upregulates Par-4 mRNA and protein levels in parallel levels of phosphorylated Smad2 and IκB-α increase. Disruption of TGF-β signaling by using ALK5 inhibitor, neutralizing TGF-β antibody or phosphoinositide 3-kinase inhibitor reduces endogenous Par-4 levels, suggesting that both Smad and NF-κB pathways are involved in TGF-β-mediated Par-4 upregulation. NF-κB-binding sites in Par-4 promoter have previously been reported; however, using chromatin immunoprecipitation assay we showed that Par-4 promoter region also contains Smad4-binding site. Furthermore, TGF-β promotes nuclear localization of Par-4. Prolonged TGF-β3 treatment disrupts epithelial cell morphology, promotes cell motility and induces upregulation of Snail, vimentin, zinc-finger E-box binding homeobox 1 and N-Cadherin and downregulation of Claudin-1 and E-Cadherin. Forced expression of Par-4, results in the upregulation of vimentin and Snail expression together with increase in cell migration. In contrast, small interfering RNA-mediated silencing of Par-4 expression results in decrease of vimentin and Snail expression and prevents TGF-β-induced EMT. We have also uncovered a role of X-linked inhibitor of apoptosis protein in the regulation of endogenous Par-4 levels through inhibition of caspase-mediated cleavage. In conclusion, our findings suggest that Par-4 is a novel and essential downstream target of TGF-β signaling and acts as an important factor during TGF-β-induced EMT.
Cell Death and Disease (2014) 5, e1044; doi:10.1038/cddis.2014.7; published online 6 February 2014
Subject Category: Cancer

In humans, majority of the solid tumors originate from epithelial cells. The invasive nature of each tumor depends on the migration capacity of epithelial cells, which they acquire via a process known as the epithelial-to-mesenchymal transition (EMT).[1] EMT is a complex process in which epithelial cells acquire mesenchymal cell-like properties through changes in cell morphology, cell–cell and cell–matrix adhesion, transcriptional regulation and migration capacity.[2,3] Members of the transforming growth factor-β (TGF-β) family have been identified as important inducers of EMT during development as well as carcinogenesis.[4,5]

TGF-β is secreted by many cells types[6–8] and directly stimulates the cellular production of extracellular matrix and microenvironment molecules in both normal and cancer cells.[9–11] The growth inhibitory properties of TGF-β have been appreciated for a long time. Indeed, several studies have shown that during early stages of carcinogenesis, TGF-β acts as a tumor suppressor principally through its ability to promote cell cycle arrest or apoptosis.[12] However, when the tumor progresses, TGF-β shifts its role from tumor suppressor to tumor promoter, inducing neoplastic cell invasiveness and metastasis through EMT and via its reprogramming of cell microenvironments.[13,14] EMT is characterized by the down-regulation of the expression of epithelial markers such as E-cadherin, which is critical in mediating epithelial cell integrity and cell–cell adhesion[15] and the upregulation of mesenchymal markers N-cadherin, which has been linked to elevated cell motility and invasive phenotype.[1,3] TGF-β stimulation of EMT is mostly achieved through its ability to induce the expression of the Snail/ZEB family of basic helix–loop–helix transcription factors, including that of Snail1, zinc-finger E-box binding homeobox 1 (ZEB1), Snail2/Slug, Twist and ZEB2/SIP1.[2,4,15,16] In light of its role as a master regulator of EMT, TGF-β stimulus also upregulates the expression

of intermediate filament protein vimentin, which is known to be expressed in all primitive cell types, but not in their differentiated counterparts.[17] In spite of all these studies, much remains to be determined regarding the molecular and genetic events involving TGF-β in the induction of EMT.

The effects of TGF-β are mediated by three TGF-β ligands, TGF-β1, -β2 and -β3. On ligand binding, TGF-β type I and II receptor form tight complexes leading to the recruitment and phosphorylation of Smad2 and Smad3.[18] Phosphorylated Smads associate with cytoplasmic Smad4 and the complex then translocates to the nucleus to control transcription of target genes.[19] In addition to Smads, TGF-β also signals through a variety of Smad-independent signaling systems, including (a) the MAP kinases (ERK1/ERK2, p38 MAPK and JNK) and (b) the survival kinases phosphoinositide 3-kinase (PI3K)/Akt. In a process to delineate the role of TGF-β signaling in cancer progression and invasion, we have identified novel targets of TGF-β signaling in normal and cancer cells[17,20] and the list is still expanding. In the present study, we have found prostate apoptosis response-4 (Par-4) as a novel target of TGF-β signaling.

Par-4 is a pro-apoptotic, tumor suppressor protein, which is expressed ubiquitously in various tissue types, and resides in both the cytoplasm and the nucleus.[21] Consistent with its tumor suppressor role, Par-4 is shown to be downregulated in many cancers.[22–24] Overexpression of Par-4 selectively induces apoptosis in cancer cells but not in normal or immortalized cells.[21,25] Low expression of Par-4 has been reported in terminally differentiated cells suggesting that Par-4 is downregulated during differentiation (reviewed in Zhao et al.[26]). However, beyond these suggestive lines of evidence, the involvement of Par-4 in EMT remains to be explored. We have previously reported that Par-4 is a direct substrate of caspase-3, which cleaves it at the EEPD[131]↓G non-canonical cleavage site; the resulting fragment retains its apoptosis inductive capabilities. One of the most potent caspases activity inhibitor is the X-linked inhibitor of apoptosis protein (XIAP). XIAP is a member of the IAP family, which is composed of intracellular pro-survival proteins that share structural and functional similarities. The pro-survival role of XIAP has been well established and amply characterized. Its activation leads to the inhibition of caspases 3, 7 and 9, severely impairing cells ability to enter apoptosis.

Here we report for the first time a novel role of Par-4 during TGF-β-induced EMT in endometrial and cervical cancer cells. In the first part of the study, we unraveled that Par-4 is a transcriptional target of TGF-β and is upregulated during EMT. A novel Smad4-binding site has been identified in the Par-4 promoter region. Furthermore, overexpression of Par-4 results in the upregulation of Snail and vimentin expression, change in cell morphology and increase in cell migration. In contrast, small interfering RNA (siRNA)-mediated silencing of Par-4 decreases the expression of Snail and vimentin. We also demonstrated that XIAP has a pivotal role in the regulation of Par-4 protein levels and activity through the control of its caspase-mediated cleavage. Our findings suggest that TGF-β targets Par-4, which has a crucial regulatory role during cellular differentiation and EMT.

Results

TGF-β signaling upregulates Par-4 expression. As for other tumor types, TGF-β is also a key component of the endometrial tumor microenvironment, which regulates autocrine and paracrine signaling pathways between a tumor and its microenvironment. Endometrial cancer cell lines, KLE and Hec-1-A and cervical cancer cell line, HeLa, are commonly used as a model to study cancer cell signaling and EMT; we also used human immortalized endometrial stromal cells (Hiesc) to assess whether the observed mechanisms were applicable to normal cells in addition to the malignant context. Furthermore, we used SKOV-3 cells, an ovarian adenocarcinoma, as well as MCF7, a breast adenocarcinoma of luminal origin. This allowed us to broaden the conclusions of the study as the results we would obtain would be widely applicable to a number of gynecological cancers. As the cells used in the present study constitutively produce the precursor protein of TGF-β isoforms and express abundant levels of TGF-β receptors[27–29] (Supplementary Figure S1C), they are a valuable model for studying autocrine and paracrine TGF-β signaling. It has been demonstrated that TGF-β acts as a tumor suppressor during the early stages of tumor; the mechanisms involved in these pro-apoptotic responses are diverse and cell type dependent. In the present study, we tested whether these actions of TGF-β occur through the regulation of pro-apoptotic protein Par-4. The results showed that exogenous TGF-β treatment upregulated Par-4 protein content in all the cell lines (Figure 1a, Supplementary Figure S1A) suggesting that the regulation of Par-4 by TGF-β is not tissue specific. In addition, TGF-β also regulates Par-4 expression at the transcript level as shown by our qRT-PCR analysis (Figure 1b, Supplementary Figure S1B) strongly supporting that Par-4 could be a novel target of TGF-β signaling.

TGF-β-mediated Par-4 upregulation occurs through both Smad-dependent and Smad-independent pathways. TGF-β signaling occurs through canonical (Smad-dependent) and/or non-canonical (Smad-independent) pathways. Therefore, we further investigated whether TGF-β signal is predominantly delivered via Smad-dependent and/or Smad-independent pathways. Western blot analysis revealed that TGF-β treatment increased Smad2 phosphorylation (Figure 2a). Previously, we have shown that TGF-β upregulates XIAP through the activation of NF-κB.[17] As the phosphorylation of IκB-α leads to the activation and nuclear translocation of NF-κB, we thus tested whether TGF-β treatment increase IκB-α phosphorylation. The results showed that IκB-α is rapidly phosphorylated following TGF-β treatment (Figure 2b). MCF7 cells did not display increased Smad nor IκB-α phosphorylation, suggesting that TGF-β signals through alternative pathways in these cells; this is supported by the fact that we observed increased Par-4 protein levels as well as mRNA independently from both cascade activation. These results suggest that TGF-β signals through both Smad-dependent and Smad-independent pathways.

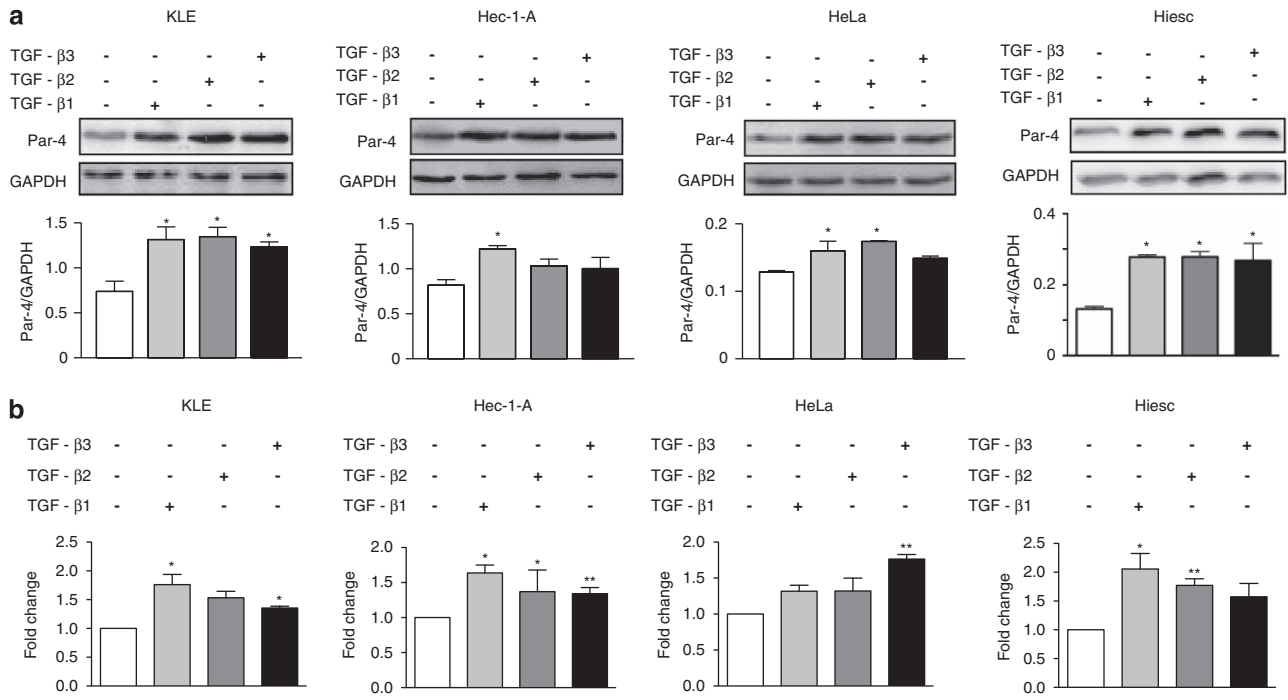Because paracrine TGF-β upregulates Par-4 expression, next we sought to determine whether autocrine TGF-β

a

b

Figure 1 TGF-β signaling upregulates Par-4 expression. (**a**) Cells were treated with different isoforms of TGF-β (10 ng/ml) for 24 h. Total proteins were extracted for western blot analysis using Par-4 antibody. GAPDH was used as a loading control. Densitometric analyses of Par-4 protein levels are presented as mean ± S.D. *P < 0.05 compared with vehicle-treated cells. (**b**) qRT-PCR analysis of transcript levels of Par-4 after TGF-β treatment; 18s rRNA was used as the reference gene. Densitometric analyses of Par-4 transcript levels are presented as mean ± S.D. *P < 0.05, **P < 0.01 compared with vehicle-treated cells

a

b
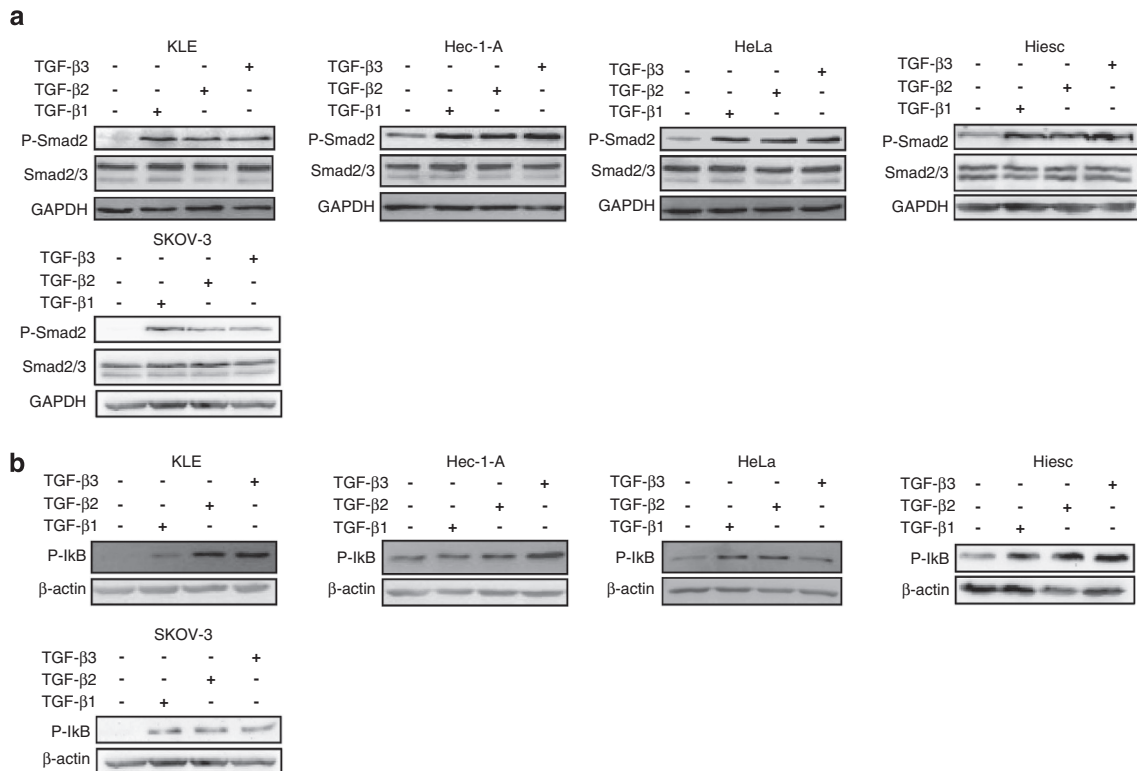
Figure 2 TGF-β regulates Par-4 expression by activating Smad and/or NF-κB pathways. (**a**) Cells were treated with different isoforms of TGF-β (10 ng/ml) for 24 h. Activation of Smad2 was analyzed using P-Smad2 antibody. GAPDH was used as a loading control. (**b**) Cells were treated with different isoforms of TGF-β (10 ng/ml) for 24 h. Activation of NF-κB pathway was analyzed by IκB-α phosphorylatin. β-actin was used as a loading control

signaling has the same effect on Par-4 levels. HeLa cells were transiently transfected with empty (pcDNA3.1) and TGF-β3 (pcDNA3.1-TGF-β3) plasmids and protein levels were analyzed by western blotting. As shown in Figure 3a, Par-4 was found to be significantly upregulated in TGF-β3 transfected cells compared with empty vector transfected cells. Autocrine TGF-β signaling occurs in endometrial and cervical cancer cells;[17] therefore, we tested whether blockade of autocrine TGF-β signaling affects endogenous Par-4 levels. First we used SB431542 (Alk5 inhibitor) that was identified as an inhibitor of the TGF-β type I receptor (activin receptor-like kinase, Alk5[30] to block autocrine TGF-β signaling. Treatment with Alk5 inhibitor in HeLa cells blocked constitutive TGF-β signaling as shown by decreased levels of phosphorylated

Smad2, in parallel it also decreased Par-4 protein levels (Figure 3b). Identical results were also observed in Hec-1-A cells (Supplementary Material Supplementary Figure S2A). Similarly, blocking TGF-β receptor signaling using neutralizing TGF-β antibody reduced endogenous Par-4 protein levels in HeLa cells (Figure 3c). These results demonstrate that autocrine TGF-β signaling constitutively regulates endogenous Par-4. In addition to Smads, we have previously shown that TGF-β also signals through PI3K/Akt and ERK. In light of the above results shown in Figure 2b that each TGF-β isoform induces IκB-α phosphorylation and the fact that IκB-α is a substrate of PI3K/Akt, and activation of PI3K/Akt therefore stimulates NF-κB activity, we verified whether blocking PI3K/Akt pathway is sufficient to block Par-4 upregulation.

Figure 3 Blocking TGF-β signaling prevents Par-4 upregulation. (**a**) HeLa cells were transiently transfected with 2 μg of empty or TGF-β3 expression vector. After 48 h of transfection, proteins were analyzed by immunoblotting using antibodies against TGF-β3, Par-4, P-Smad2, total Smad2 and GAPDH. Densitometric analyses of Par-4 and P-Smad2 protein levels are presented as mean ± S.D. *P<0.05 compared with vehicle-treated cells. (**b**) HeLa ce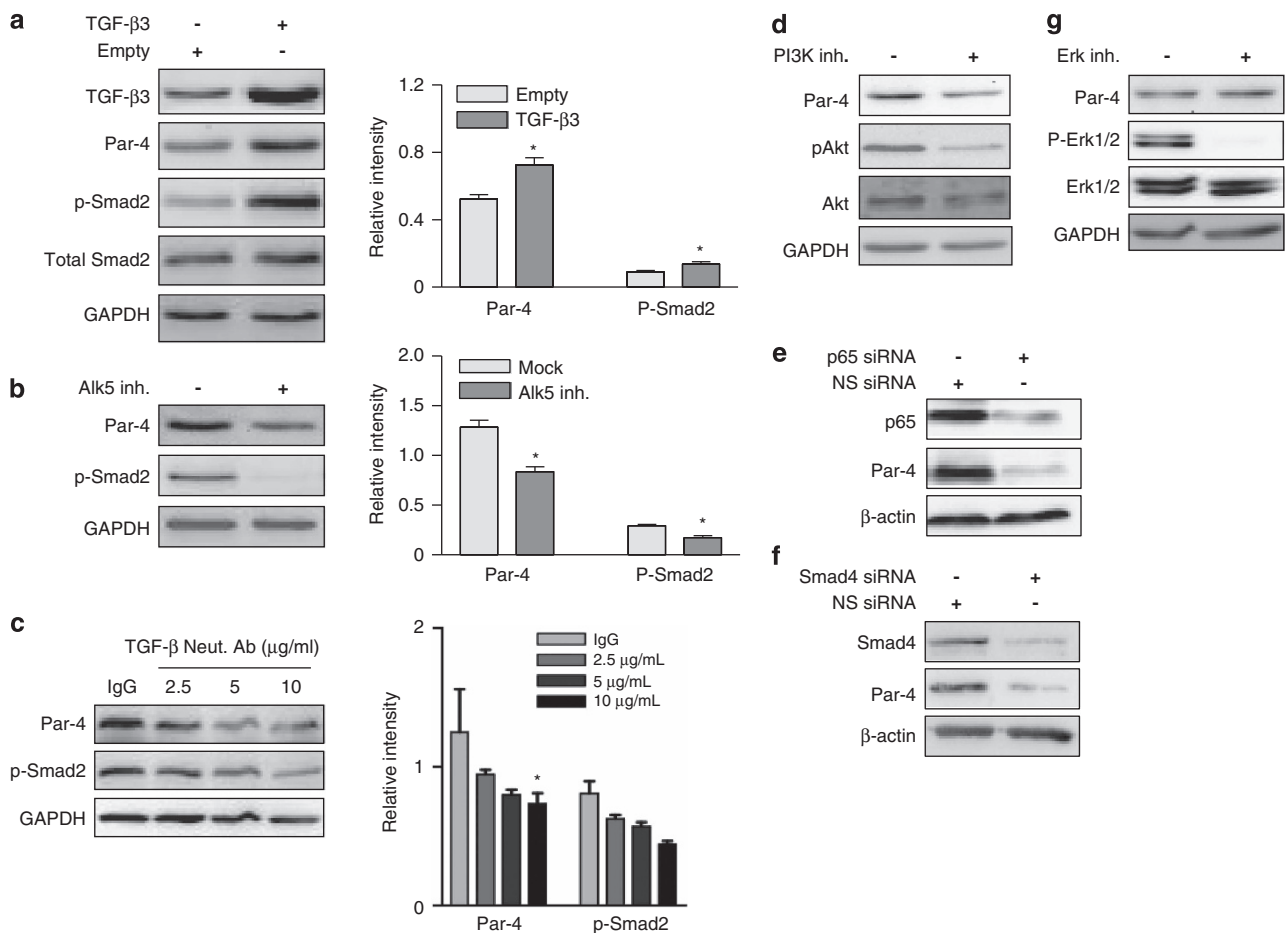lls were treated with 50 μm Alk5 inhibitor (SB431542) or vehicle for 24 h, and Par-4 protein levels were determined using western blotting. Levels of P-Smad2 were determined to monitor the efficiency of TGF-β pathway inhibition. GAPDH was used as a loading control. Densitometric analyses of Par-4 and P-Smad2 protein levels are presented as mean ± S.D. *P<0.05 compared with vehicle-treated cells. (**c**) HeLa cells were treated with anti-TGF-β neutralizing antibody (2.5, 5 and 10 μg/ml) or isotypic control antibody for 24 h, and Par-4 protein levels were determined using western blotting. Levels of P-Smad2 were determined to monitor the efficiency of TGF-β pathway inhibition. GAPDH was used as a loading control. Densitometric analyses of Par-4 and P-Smad2 protein levels are presented as mean ± S.D. *P<0.05 compared with vehicle-treated cells. (**d**) HeLa cells were treated with 50 μM PI3K inhibitor LY294002 or vehicle for 1 h. Par-4 protein levels were determined using western blotting. Levels of P-Akt were determined to monitor the efficiency of PI3K inhibitor. GAPDH was used as a loading control. (**e**) HeLa cells were transiently transfected with 50 nM of scrambled or p65-specific siRNA. After 48 h, proteins were analyzed by immunoblotting using antibodies against p65 and Par-4. β-actin was used as loading control. (**f**) HeLa cells were transiently transfected with 100 nM of scrambled or Smad4-specific siRNA. After 48 h, proteins were analyzed by immunoblotting using antibodies against Smad4 and Par-4. β-actin was used as loading control. (**g**) HeLa cells were treated with 40 μM MEK1/2 inhibitor U0126 for 1 h. Par-4 protein levels were determined using western blotting. Levels of phosphorylated ERK1/2 were determined to monitor the efficiency of MEK inhibitor. GAPDH was used as a loading control

We used PI3K inhibitor, LY294002, to inhibit PI3K/Akt signaling. The results demonstrate that treatment with LY294002 decreased Par-4 levels, suggesting that Par-4 is indeed regulated by the activation of NF-κB signaling cascade in HeLa cells (Figure 3d). Using the same model, we then reduced p65 levels through siRNA to confirm this observation. The results corroborated those obtained through the inhibition of PI3K/Akt pathway by LY294002, demonstrating that the NF-κB pathway was indeed involved in Par-4 regulation (Figure 3e). We used a similar approach to demonstrate the involvement of Smad signaling in Par-4 expression. We used a Smad4 siRNA to reduce its expression and found endogenous levels of Par-4 to be reduced (Figure 3f). In contrast, treatment with U0126 (a highly selective inhibitor of both MEK1 and MEK2) did not have any effect on Par-4 levels (Figure 3g). Taken together, these results implied that TGF-β regulates Par-4 levels through Smad and NF-κB activation.

Par-4 promoter region contains Smad-binding elements (SBE). NF-κB responsive elements in the Par-4 promoter region have previously been reported.[31] Therefore, NF-κB activation mediated by IκB-α phosphorylation in the present study could arbitrate the transcriptional upregulation of Par-4 by TGF-β. With the knowledge that Smads are also known to interact directly with SBE in the promoter regions of the target genes, we searched for the presence of SBE in the promoter of Par-4 using a chromatin immunoprecipitation (ChIP)-PCR approach. Chromatin from the TGF-β-treated and -untreated HeLa cells was immunoprecipitated using specific antibody against Smad4. Genomic DNA fragments bound to Smad4 were analyzed by PCR using random primers (P1 and P2) designed to include conserved SBE (P1: 5'-GTCT-3' at -1742 to -1739) or (P2: 5'-AGAC-3' at -1510 to -1507) in Par-4 promoter region (Figure 4a). Analysis of genomic DNA immunoprecipitated with Smad4 and RNAPolII antibody efficiently recovered Par-4 promoter from both TGF-β-treated and -untreated HeLa cells (Figure4b, lane 2 and 3) suggesting paracrine and autocrine TGF-β signaling occurs in these cells. Interestingly, Smad4 was found to bind at both the predicted SBE using primer P1 and P2. No genomic DNA was pulled out in immunoprecipitates from rabbit or mouse IgGs (Figure 4b lane 1 and 5). These results demonstrate that Smads indeed interact with the Par-4 promoter. All together, these findings strongly support the idea that Par-4 is upregulated by TGF-β through both the NF-κB pathway and Smad pathway.

Par-4 expression is increased during TGF-β-induced EMT. Previous studies hinted at the ability of TGF-β to induce EMT in endometrial cells.[32] However, a deeper analysis seemed necessary to confirm TGF-β role in the enactment of this mechanism. We treated various endometrial cells with all three isoforms of TGF-β and examined the regulation of classical EMT markers. As shown in Figure 5a, HeLa cells displayed an upregulation of the N-Cadherin, an important marker of EMT; both the Snail and vimentin levels were also increased. Similar results were observed in Hiesc, KLE and SKOV-3 cell lines. They displayed a pronounced shift in cadherins expression, one of the hallmarks of EMT as well as an upregulation of Snail. MCF7 cells did not show
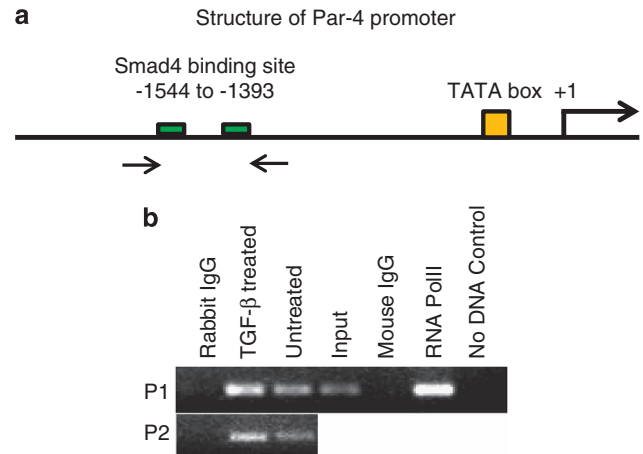

Figure 4 (**a**) P1 and P2 indicate the PCR primer sets used for ChIP assays. (**b**) HeLa cells were treated with TGF-β3 (10 ng/ml) for 24 h. Chromatin DNA was immunoprecipitated using specific antibody against Smad4. An antibody to RNA polymerase II (RNAPolII) is used as a positive control and normal rabbit IgG/mouse IgG served as a negative control. DNA fragments were amplified with primers P1 and P2 specific for Par-4 promoter. Lane 1, rabbit IgG; lane2, TGF-β3 treated cells; lane 3, untreated cells; lane 4, input (10% sonicated chromatin DNA). 'Input' indicates control PCR and shows the amount of Par-4 promoter DNA present in each sample before ChIP. Lane 5, mouse IgG; lane 6, RNAPolII, lane7, no DNA PCR control. ChIP-PCR products for Par-4 promoter were observed in anti-Smad4 ChIP (lane 2 and 3), input (lane 4) and anti-RNA polymerase II ChIP (positive control, (lane 6))

enhanced Snail expression or changes in their cadherin profile. However, they exhibited drastically reduced claudin-1 expression, which is an indicator of metastatic potential and poor prognosis[33–36] (Supplementary Figure S2B). Taken together, these results suggest that TGF-β induces EMT in both uterine and ovarian cells as well as promote metastatis and tumor progression through the loss of claudin-1 in luminal breast cancer cells. These results were also confirmed by autocrine TGF-β3 signaling by transfecting HeLa and KLE cells with TGF-β3 plasmid. The results demonstrate that overexpression of TGF-β3 induces expression of vimentin and transcriptional factors, Snail and ZEB1. In addition, there was a decrease in the expression of claudin-1. In parallel, Par-4 was found to be upregulated (Figure 5b). To support these observations, we further analyzed TGF-β's ability to induce morphological changes characteristic of EMT. As shown in Figure 5c, confocal microscopy examination revealed that treatments with each TGF-β isoforms induces a drastic alteration in HeLa cell shape; whereas, untreated cells display the typical cobble-stone-like epithelial characteristics phenotype, a 24-h treatment with all three TGF-β isoforms induced an elongated and spindle shaped phenotypic characteristics of fibroblasts. This effect was most evident in TGF-β3-treated cells. Similar changes in cell morphology were observed in both KLE and SKOV-3 cells using TGF-β3 (Supplementary Material Supplementary Figure S2C). Besides inducing the morphological characteristics of EMT, TGF-β treatment also resulted in behavioral changes that are associated with EMT, such as an increase in cell motility and invasion. We have observed that the cell migration ability of HeLa cells was increased

following TGF-β stimulation with each isoform (Figure 5d). Prolonged exposure of the cells to TGF-β3 induced upregulation of various EMT markers as well as a progressive increase of Par-4 in a similar fashion (Supplementary Figures S2D and E). Together, these suggest that TGF-β induces EMT in multiple cell lines, a process in which Par-4 has a potential role.

Par-4 directly upregulates other EMT inducers. To address the potential relationship between Par-4 and other transcription factors and signaling molecules implicated in EMT, we tested whether Par-4 itself induces the expression of known EMT markers. HeLa cells were transiently transfected with Myc-tagged Par-4 plasmid followed by immunoblotting. The results showed that Par-4 increased endogenous protein levels of N-cadherin, vimentin and Snail (Figure 6a). Similar results were found in SKOV-3 cells. Interestingly, Par-4 reduced claudin-1 protein levels,

similar to the results obtained with TGF-β treatments (Supplementary Figure S3A). This suggests that Par-4 alone is sufficient to reduce claudin expression in MCF7 cells. Observations made in HeLa cells were further validated using immunofluorescence microscopy. It is evident from Figure 6b that Par-4 overexpression induced vimentin expression and the cells acquired elongated shape, which is a characteristic feature of EMT. In contrast, knockdown of Par-4 using siRNA downregulated vimentin and Snail protein levels (Figure 6c). Using transwell migration assay, we observed that Par-4 overexpression also enhances cell migration (Figure 6d). We then proceeded to assess the effect of Par-4 knockdown concurrent with exogenous TGF-β treatments to determine whether Par-4 was necessary for TGF-β to induce EMT characteristics. Both HeLa and SKOV-3 cells were subjected to Par-4 knockdown using siRNA as well as TGF-β3 treatments. We observed that TGF-β3 was unable to induce enhanced Snail expression in the absence
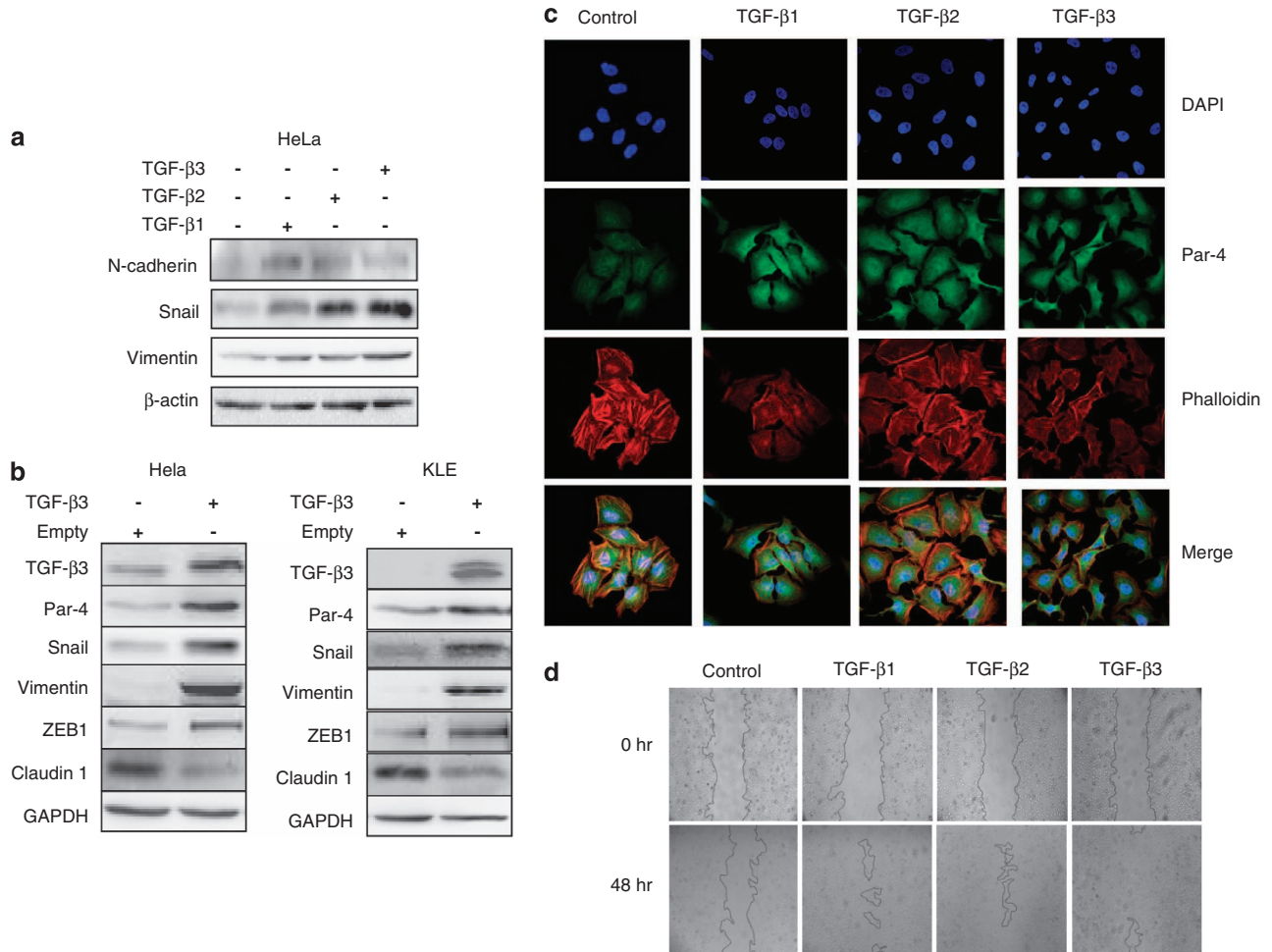

Figure 5 TGF-β induces upregulation of Par-4 concomitant with EMT. (**a**) HeLa cells were treated with different isoforms of TGF-β (10 ng/ml) for 48 h. Total proteins were extracted for western blot analysis using N-Cadherin, vimentin and Snail antibody. β-actin was used as a loading control. (**b**) HeLa and KLE cells were transiently transfected with 2 μg of empty or TGF-β3 expression vector. After 48 h of transfection, proteins were analyzed by immunoblotting using antibodies against TGF-β3, Par-4, Snail, vimentin, ZEB1 and claudin-1. GAPDH was used as a loading control. (**c**) HeLa cells were treated with different isoforms of TGF-β (10 ng/ml) for 48 h. Cells were analyzed for morphological changes by confocal microscopy. Magnification used was × 60 with oil emersion. (**d**) Equal number of HeLa cells seeded in 6-well plates. After 24 h, cell monolayer was scratched to create a wound and treated with different isoforms of TGF-β (10 ng/ml) for 24 and 48 h. Wound closure was analyzed by microscopy using × 10 magnification
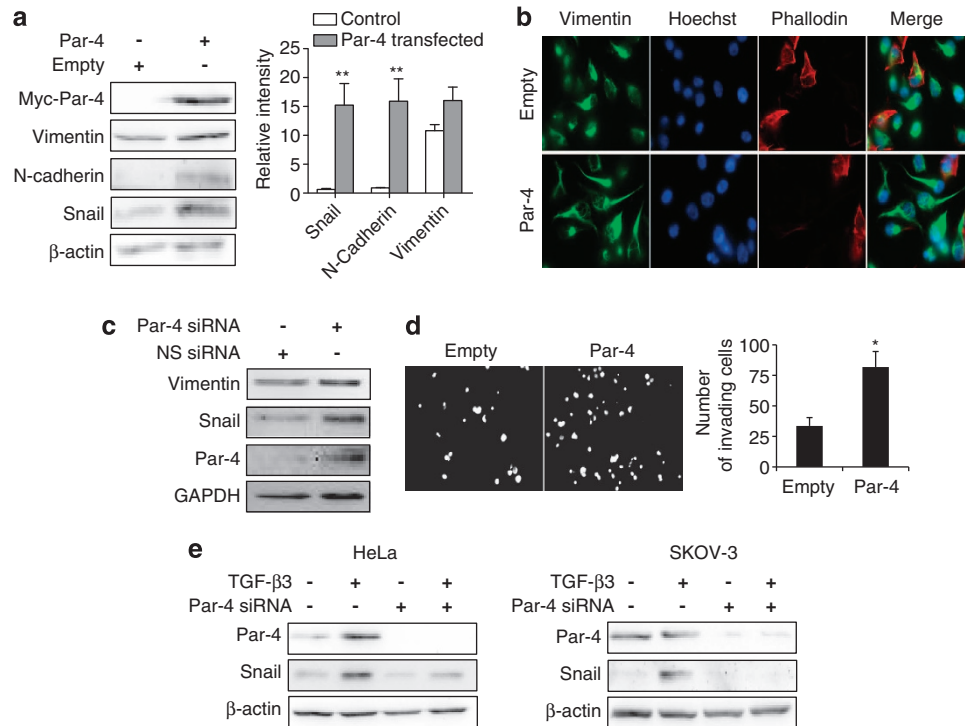
Figure 6 Par-4 regulates EMT. (**a**) HeLa cells were transiently transfected with 2 μg of the empty or Par-4 in pCMV entry-Myc-DDK vector. After 48 h, total cell lysates were analyzed for vimentin, Snail and N-cadherin protein levels by western blotting. Anti-Myc tag antibody was used to reveal the extent of Par-4 overexpression. β-actin was used as a loading control. Densitometric analyses of protein levels are presented as mean ± S.D. **$P < 0.01$ compared with empty plasmid transfected cells. (**b**) HeLa cells were transiently transfected with 2 μg of the empty or Par-4 in pCMV entry-Myc-DDK vector. After 48 h, cells were subjected to immunofluorescence for vimentin (Alexa Fluor 594, green). The nuclei were stained with Hoechst 33258 (blue), and phalloidin (red), which stains the actin cytoskeleton, is used to visualize the shape and integrity of the cells. Magnification, × 63. (**c**) HeLa cells were transfected with Par-4 siRNA or control nonsilencing (NS) siRNA. After 48 h, cells were collected for western blot analysis using Par-4, Snail and vimentin antibodies. GAPDH was used as a loading control. (**d**) HeLa cells were transiently transfected with 2 μg of the empty or Par-4 in pCMV entry-Myc-DDK vector. After 48 h, cells were trypsinized and placed in matrigel-coated transwell filter chambers and incubated for 24 h. The noninvading cells were removed from the upper surface of the membrane, cells that adhered to the lower surface of the filter were fixed, and the nuclei were stained with Hoechst 33258 and analyzed by fluorescence microscopy. Magnification, × 10. Histogram shows number of cells invading matrigel from three independent experiments. Nuclei were counted from five different fields in each experiment. *$P < 0.05$. (**e**) HeLa and SKOV-3 cells were transfected with Par-4 siRNA or control nonsilencing (NS) siRNA as well as TGF-β3. After 48 h, cells were collected for western blot analysis using Par-4 and Snail antibodies. β-actin was used as a loading control

of Par-4, further confirming its crucial role in TGF-β-mediated EMT (Figure 6e). Taken together, the data suggest that upregulation of Par-4 in response to TGF-β has an essential role in the inducement of EMT.

XIAP regulates Par-4 cleavage in normal and malignant cells. We have previously established that TGF-β upregulates XIAP and recently we have also evidenced that cleavage of Par-4 by caspase-3 is required to potentiate its pro-apoptotic activity.[37] Present study also evidenced that TGF-β was a crucial regulator of Par-4 levels. We thus sought to understand the relationship between Par-4 and XIAP. We first used primary mouse embryonic fibroblasts (MEFs) derived from genetically engineered XIAP knockout (XIAP$^{-/-}$) mice or from control (XIAP$^{+/+}$) mice to investigate whether XIAP regulates Par-4 protein *in vivo*. High levels of Par-4 were found in XIAP$^{+/+}$ cells compared with XIAP$^{-/-}$ cells (Figure 7a) suggesting that XIAP constitutively regulates Par-4 levels in resting cells. Further, we endeavored to understand the process by which XIAP regulates Par-4 levels. We thus investigated whether XIAP regulatesPar-4 through the control of its cleavage. Wild type (WT) and XIAP knockout MEF cells were treated with

cisplatin to induce apoptosis and thus Par-4 cleavage. We found that XIAP$^{+/+}$ cells failed to cleave Par-4 when treated with cisplatin; however, the knockout of XIAP restored the ability of MEF cells to cleave Par-4. We also observed an increased level of cleaved caspase-3 as well as a lowered level of full length Par-4 (Figure 7b). To further understand the mechanism by which XIAP controls Par-4 cleavage, we used HeLa cells transfected with XIAP constructs (Myc$_6$-XIAP (WT), Myc$_6$-XIAP-H467A (inactive mutant), or empty vector. These transfections were followed by cisplatin treatment to induce apoptosis. Using this approach, we found that caspase-3-mediated Par-4 cleavage was completely abrogated in WT XIAP overexpressing cells and not in mutant XIAP expressing cells, suggesting that XIAP RING domain is necessary for the control of Par-4 cleavage (Figure 7c). The obtained results validated XIAP as a key regulator of Par-4 protein levels, in both normal and malignant cells, through the control of its cleavage.

Par-4 cleavage inhibits its ability to induce increased cell motility and EMT-like characteristics. TGF-β induces apoptosis in a variety of cell types; in contrast, we have previously reported that TGF-β is unable to trigger apoptosis
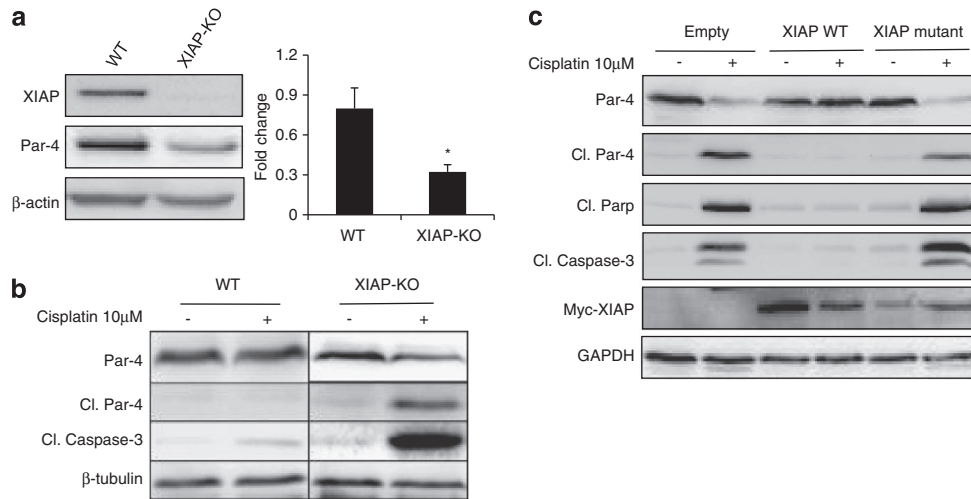
Figure 7 XIAP regulates Par-4 protein levels through the control of its cleavage. (**a**) Total proteins were collected from primary MEFs derived from XIAP$^{+/+}$ and XIAP$^{-/-}$ mice and Par-4 protein levels were determined using western blotting. Densitometric analysis of Par-4 protein levels is presented as mean ± S.D. *, $P < 0.05$. β-actin was used as a loading control. (**b**) HeLa cells were transiently transfected with 1 μg of control plasmid (pcDNA3; empty), mutant Myc$_6$-XIAP-H467A plasmid (XIAP mutant) or Myc$_6$-XIAP WT plasmid (XIAP WT) using Fugene 6. After 48 h, cells were incubated in the presence or absence of 10 μM cisplatin. Following cisplatin treatment for 24 h, cells were collected for western blotting. Membranes were probed using antibodies against Par-4, Myc tag (for XIAP). Cleaved PARP and cleaved caspase-3 antibodies were used to monitor caspase-3 activation. GAPDH was used as loading control. (**c**) Primary MEFs derived from XIAP$^{+/+}$ and XIAP$^{-/-}$ mice were treated with 10 μM cisplatin for 24 h. Cells were collected and western blotting was performed using antibodies against Par-4 and cleaved caspase-3. β-tubulin was used as a loading control

in endometrial cancer cells under similar conditions.[27] Given that TGF-β upregulates Par-4, which is a known pro-apoptotic protein, it was surprising that the cells did not undergo apoptosis. Previous experiments demonstrated that XIAP regulated Par-4 levels through the regulation of its caspase-3-mediated cleavage. We sought to understand whether this mechanism could explain the change in Par-4 effect from tumor suppressor to EMT inducer. We hypothesized that the inhibition of Par-4 cleavage would limit its ability to induce apoptosis and increase its EMT inducing capabilities. We transfected both HeLa (Figure 8a) and Hiesc (Figure 8b) cells with XIAP siRNA, followed by a transfection of either full length Par-4 or empty vector. The Par-4 transfected cells demonstrated highly enhanced motility and acquired morphological characteristics typical of cells undergoing EMT such as elongation, spindle-like appendages and general fibroblastic morphology. This correlated with previous observations. However, cells transfected with both Par-4 expression plasmid and XIAP siRNA did not display EMT-like morphology (Figure 8c) and did not acquire heightened motility. Altogether, these results support the idea that Par-4 is a pivotal effector of EMT whose effect is regulated by its cleavage, a mechanism on which XIAP exerts a control through caspases inhibition.

Discussion

The TGF-β signaling pathway governs multiple biological processes through the regulation of various target genes. However, alterations or genetic mutations in TGF-β signaling often lose its growth inhibitory properties and thus making room for cancer cells to proliferate, invade and metastasize during tumor progression. EMT is an important event in tumor progression, which leads to cell invasion and metastasis. By activating both Smad-dependent and Smad-independent

pathways, TGF-β acts as a potent inducer of EMT.[4,5] Despite the greater understanding and identification of TGF-β responsive genes, knowledge gap remains as to what controls the switching of roles from tumor suppressor to a tumor promoter. In the present study we have identified Par-4 as a target of TGF-β signaling and demonstrated its role during TGF-β-induced EMT (Supplementary Figure S4).

Previous studies have demonstrated an induction of Par-4 expression in response to diverse apoptotic stimuli. Although endogenous Par-4 itself does not induce apoptosis, yet it is important for apoptosis induced by exogenous cytotoxic insults. Currently, what regulates Par-4 expression is still under investigation. The present study provides the first evidence that TGF-β can induce Par-4 at both transcript and translational level. Both Smad and NF-κB signaling pathways were found to be involved in TGF-β-mediated Par-4 upregulation. Previously, NF-κB responsive elements have been evidenced in the Par-4 promoter region, which leads to the NF-κB-dependent transactivation of Par-4.[31] Herein, we confirm that Par-4 expression is regulated by NF-κB, but most importantly, using a ChIP-PCR approach, we uncovered Smad4-binding elements in Par-4 promoter region.

Identification of the target genes of Smad4 has been reported in both normal epithelial and cancer cells.[38] Originally, Zawel et al.[39] identified an 8-bp palindromic sequence 5′-GTCTAGAC-3′ as the SBE particularly in case of Smad3 and Smad4 and later it was shown that 5′-GTCT-3′ or its complement 5′-AGAC-3′ alone can also act as SBE. Interestingly, CAGA is also recognized to mediate binding to Smad3 and Smad4, and are required for TGF-β-induced transcriptional activation of the plasminogen activator inhibitor-1 promoter.[40] Later studies have suggested that in addition to the GTCT and AGAC elements, Smad4 is also able to recognize a GC-rich sequence.[41,42] It is important to note
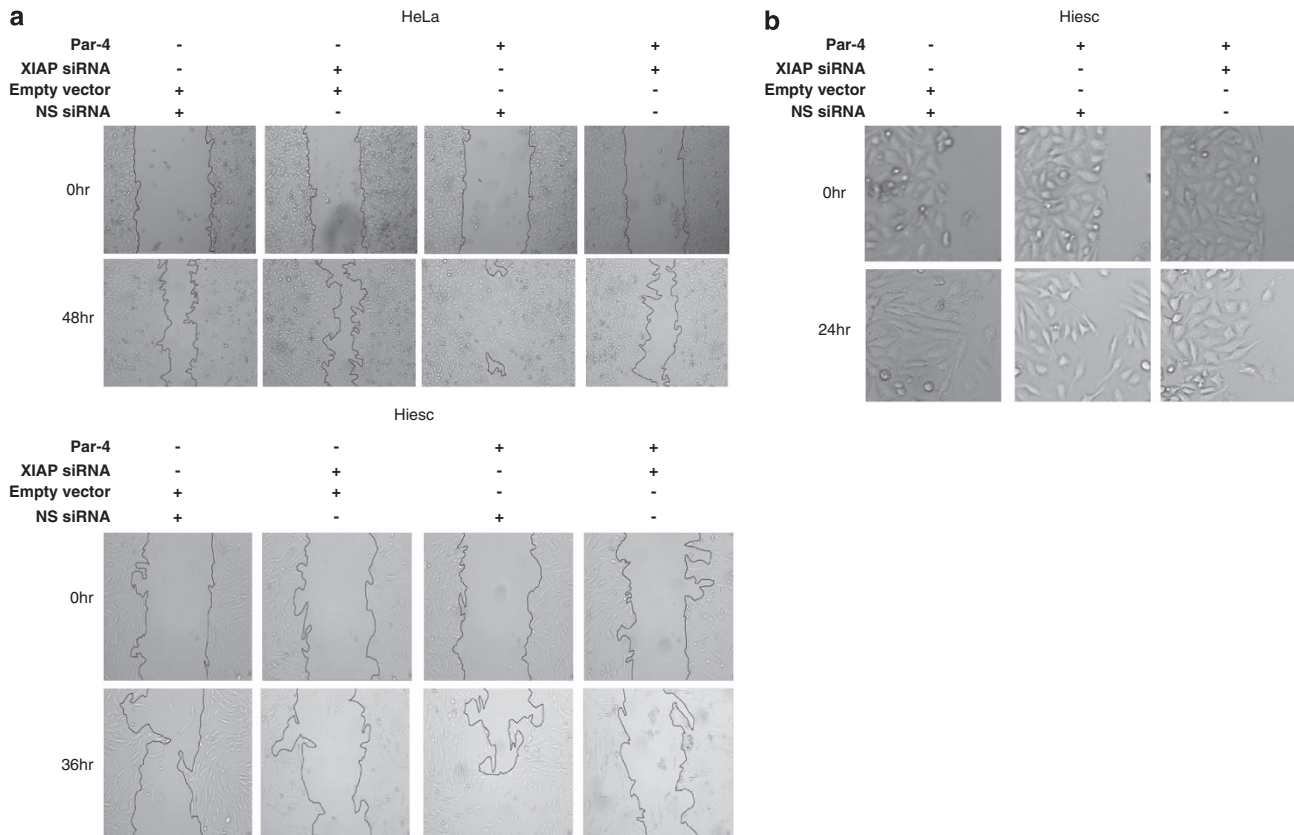
Figure 8 Par-4 cleavage inhibits its ability to induce motility and morphological changes. (**a**) Equal number of HeLa and Hiesc cells were seeded in 6-well plates and allowed to grow for 24 h. Cells were then transfected with XIAP siRNA for a period of 6 h at the end of which they were transfected with a Par-4 expression plasmid. Cells were then allowed to grow for an additional 18 h; the media was then changed and the cell monolayer was wounded with a plastic tip. This was considered as time 0. Cells were then observed every 12 h. Wound closure was analyzed by microscopy using × 10 magnification (**b**) HeLa cells morphology before and after transfections at × 10 magnification

that Par-4 promoter sequence is extremely GC-rich. A careful examination of the Par-4 promoter region revealed many potentially important SBE or SBE-like sequence motifs. We have identified that Par-4 contains two SBE located at − 1742 to − 1739 (5′-GTCT-3′) and − 1510 to − 1507 (5′-AGAC-3′). One of these sites (− 1742 to − 1739) contains a perfect Smad box (GTCT). Interestingly, the other consensus sequence: − 1510 to − 1507 (5′-AGAC-3′) is similar to the SBE found in the promoter region of TGF-β target genes, such as α2(I) collagen, and germline Igα constant region.[43] In addition to the two SBE we have identified here, Par-4 promoter contains many regions that can mediate TGF-β responses through Smad binding. Previously it has been suggested that one or more SBE could be present in many Smad-responsive promoter regions.[43]

Surprisingly, while Par-4 was being upregulated by TGF-β, cells were not undergoing apoptosis.[27] In a previous study, we have reported that XIAP is also a transcriptional target of TGF-β signaling.[17] As caspase-3-mediated cleavage of Par-4 potentiates its apoptotic activity, we found that XIAP prevents cleavage of Par-4 by caspase-3 thus promoting the accumulation of the uncleaved form of the protein. Furthermore, a low level of Par-4 in XIAP KO MEFs implies that XIAP also regulates endogenous levels of Par-4. Solid evidence is available in literature regarding Par-4 as a negative regulator of XIAP through inhibition of ζPKC–NF-κB pathway.[44]

All together this implies that a negative feedback loop exists between the regulation of Par-4 and XIAP.

Tumor suppressor role of Par-4 is well established based on the fact that Par-4 is downregulated in various types of tumors. Our data demonstrating a novel role of Par-4 during EMT suggest that Par-4 could also function as a tumor promoter thus contradicting its reported tumor suppressor activity. However, it is possible that similar to TGF-β, Par-4 has a dual role during tumorigenesis. The possible mechanism by which Par-4 mediates TGF-β-induced EMT likely involves an association with WT1 and/or aPKC. Par-4 has previously been shown to physically interact with WT1 and aPKC in the nucleus. In the present study, Par-4 was found to accumulate in the nuclear extracts following TGF-β treatment (Supplementary Figures S3B and C) suggesting that, on TGF-β stimulation, Par-4 readily translocates to the nucleus. Interestingly, WT1 was shown to regulate EMT by upregulating Snail and downregulating E-cadherin by binding to their promoters.[45] Thus our results herein demonstrating that Par-4 accumulates in the nucleus and upregulates Snail led us to speculate that Par-4, which is a binding partner for WT1, may act as a transcriptional activator of WT1 and thus could promote EMT. The absence of enhanced Snail expression following TGF-β treatments or Par-4 transfection in MCF7 cells could explain the lack of changes in these cells cadherin expression profile. Multiple articles report MCF7 as

10

Snail-negative cells;[46,47] the exogenous expression of this gene generally induced EMT characteristics in MCF7. However, our study demonstrates that Par-4 upregulation could be directly responsible for TGF-β-mediated claudin-1 downregulation; this loss of expression is of critical importance in the establishment of metastatic tumorigenesis, as widely reported by the literature.[33,35,36] It is also the hallmark of the claudin-low breast cancer subtype.[48] Because of the presence of leucine zipper domain at the C terminus, it will be interesting to determine if Par-4 can itself act as a transcription factor to exert a specific function during EMT. Concerning the involvement of aPKC, recently Gunaratne et al. have specifically shown that inhibition of aPKC isoforms delays TGF-β receptor degradation and extends TGF-β-induced Smad2 signaling. Given that Par-4 inhibits aPKC, it is possible that upregulation of Par-4 following TGF-β stimulation could inhibit aPKC in the cells, which further leads to prolonged TGF-β signaling for EMT induction. Collectively, these findings highlight a broad role for Par-4 in TGF-β-induced EMT. Further studies are warranted to dissect the unraveled roles of Par-4 in tumor progression. This study establishes for the first time that Par-4 regulates EMT, the first process attributed to Par-4 that is uninvolved with apoptosis.

Materials and Methods

Cell lines and reagents. Human endometrial carcinoma cell lines, KLE and Hec-1-A, human cervical cancer cell line, HeLa, human ovarian adenocarcinoma cells, SKOV-3 and human breast luminal adenocarcinoma, MCF7, were purchased from ATCC (Manassas, VA, USA). Hiesc cells were obtained from Michel A Fortier, Université Laval.[49] Primary MEFs derived from XIAP$^{+/+}$ and XIAP$^{-/-}$ mice. All the antibodies were obtained from Cell Signaling technology (Danvers, MA, USA) except for anti-TGF-β neutralizing antibodies (Santa Cruz Biotechnology, Santa Cruz, CA, USA) and anti-rabbit secondary antibody (Bio-Rad Laboratories, Hercules, CA, USA). Recombinant TGF-β1, TGF-β2 and TGF-β3 were purchased from Calbiochem (San Diego, CA, USA). PI3K inhibitor, LY294002 and MEK inhibitor, U0126 were obtained from Cell Signaling Technology. Cisplatin and Alk5 inhibitor, SB431542 were purchased from Sigma-Aldrich (St. Louis, MO, USA).

Treatments and transfections with constructs and siRNA. Cells were seeded in 6-well plates and after 24 h, medium was replaced with fresh media containing appropriate treatment (TGF-βs, neutralizing TGF-β antibody, PI3k inhibitor, MEK inhibitor and/or Alk5 inhibitor).

Par-4 (pCMV entry-Par-4-Myc-DDK) and empty vector (pCMV entry-Myc-DDK) plasmids encoding a Myc tag at the C terminus were purchased from Origene (Rockville, MD, USA). XIAP constructs WT (Myc$_6$-XIAP WT) and mutant (Myc$_6$-XIAP-H467A, E3 ligase inactive mutant) were a kind gift from Dr. Herman H Cheung (Children's Hopital of Eastern Ontario Research Institute, Ottawa, Ontario, Canada). TGF-β3 plasmid was cloned in our lab in pcDNA3.1/V5-His TOPO-TA (Invitrogen, Carlsbad, CA, USA). One day before transfection, cells were plated at 3×10^5 per well in 6-well plates to achieve a confluency of ~70% after 24 h. Cells were transfected with 1–2 μg of expression vector using Fugene 6 (Roche, Indianapolis, IN, USA) according to the manufacturer's instructions. Plates were incubated for 48 h at 37 °C before cells were collected and subjected to further analysis.

For silencing of Par-4, XIAP, p65 and Smad4 expression, cells were seeded in 6-well plates (~3×10^5 cells per well) and after 24 h cells were transiently transfected with 50 nM (100 nM for XIAP and Smad4) Par-4/XIAP/p65-specific/Smad4 siRNA or control nonsilencing siRNA (Santa Cruz Biotechnology) using TransIT-TKO transfection reagent (Mirus, Madison, WI, USA) in accordance with the manufacturer's instructions. Plates were incubated for 48 h before cells were collected for further analysis.

Reverse transcriptase PCR (RT-PCR). Following TGF-β treatment, total RNA was isolated from the cells using TRIzol reagent (Invitrogen) according to the manufacturer's instructions. One microgram of RNA was reverse transcribed using

Moloney murine leukemia virus reverse transcriptase (Invitrogen) and oligo (dT) primers. The reverse-transcribed RNA was then amplified by PCR using specific primers against Par-4 and GAPDH as described previously.[37] The PCR products obtained were electrophoresed on a 1% agarose gel and visualized using SYBR-Safe (Invitrogen) staining.

Western blot analysis. After the end of the treatment period or transfection time, both floating and attached cells were collected and cell lysate was done using cold radioimmunoprecipitation assay lysis buffer containing protease inhibitors (Complete; Roche Applied Science, Indianapolis, IN, USA), followed by three freeze–thaw cycles. Nuclear and cytoplasmic extracts were prepared from the cells using NE-PER reagent (Pierce, Rockford, IL, USA). Proteins were measured using the Bio-Rad DC protein assay. Western blotting was performed as described.[37] Appropriate peroxidase-conjugated secondary antibodies were used, and the blot was developed using SuperSignal West Femto substrate (Thermo Scientific, Rockford, IL, USA), as described by the manufacturer.

Immunofluorescence microscopy analysis. Cells treated with growth factors or transfected with appropriate plasmids as described above were grown in 6-well plates containing sterile coverslips. On the day of analysis, cells were fixed with 4% paraformaldehyde for 10 min, and permeabilized for 10 min using 0.1% Triton X-100 in 0.1% sodium citrate at room temperature. After being blocked with Dako blocking serum for 1 h, cells were incubated with primary antibody (1 : 100 dilution) or isotypic control antibody for 1 h. After incubation with primary antibody, cells on the coverslips were washed three times with PBS and then incubated with fluorescent-tag-conjugated secondary antibodies (1 : 200 dilution) for 30 min in dark. In some experiments, Rhodamine–phalloidin, which stains the actin cytoskeleton, is used to visualize the shape and integrity of the cells. Cells were counterstained with Hoechst 33248 (0.25 μg/ml) for 5 min, and slides were mounted using Slowfade gold antifading reagent (Invitrogen) and viewed under a Carl Zeiss Axio observer Z1 microscope.

Cell migration and wound healing assay. The motility and invasive ability was evaluated using 8-μm pore size transwell inserts, which were coated with 2 mg/ml matrigel. Cells were transfected with 2 μg of empty or Par-4 plasmids. After 48 h, cells were trypsinized, resuspended in respective basal medium without serum and 2×10^5 cells were seeded in the upper chamber inserts. The lower chambers were filled with 600 μl of respective culture medium with 10% FBS. After 24 h, migration assay was terminated by removing the cells from the upper chamber of the filter. Cells that had invaded through the matrigel and adhered to the lower surface of the filter were fixed, and the nuclei were stained with Hoechst 33258 (as described above) and analyzed by fluorescence microscopy. Nuclei were counted from five different fields in each experiment.

For wound healing assay, equal numbers of cells were seeded in 6-well plates and were allowed to grow for 24 h. Cell monolayer was wounded with a plastic tip and TGF-β treatment was initiated. The migration was followed for 48 h and photomicrographs were taken with the Carl Zeiss Axio observer Z1 microscope at 0, 24 and 48 h.

ChIP assay. ChIP assays were done using an EZ CHIP kit (Upstate Biotechnology, Lake Placid, NY, USA) according to the manufacturer's instructions. Follwing TGF-β treatment, cell lysates were made. Chromatin was sonicated to obtain fragmented DNA (100–200 bp) and immunoprecipitated with control IgG (mouse and rabbit), anti-Smad4 (Cell Signaling) or anti- RNA Polymerase II (RNAPolII) (Upstate Biotechnology). The primer pairs used for ChIP assays are P1 (Fwd 5′-GAGAGGCAGAGACAGGGT-3′; Rev 5′-AAGAAAAC TGCGGTGCCCT-3′) and P2 (Fwd 5′-ATCATGTGCTACCTGGGC-3′; Rev 5′-CG CACCTAAGACTGACCT-3′). PCR was done as described previously.[37]

Statistical Analysis. Statistical analysis was done by one-way analysis of variance with Tukey's *post hoc* test or Student's *t*-test where appropriate. Statistical significance was accepted when $P < 0.05$. *$P < 0.05$; **$P < 0.01$; ***$P < 0.001$. All analysis was performed using GraphPad PRISM software, version 3.03 (GraphPad Software, Inc., La Jolla, CA, USA).

Conflict of Interest

The authors declare no conflict of interest.

1. Thiery JP. Epithelial-mesenchymal transitions in tumour progression. *Nat Rev Cancer* 2002; **2**: 442–454.
2. Zavadil J, Bitzer M, Liang D, Yang YC, Massimi A, Kneitz S *et al.* Genetic programs of epithelial cell plasticity directed by transforming growth factor-beta. *Proc Natl Acad Sci USA* 2001; **98**: 6686–6691.
3. Thiery JP, Sleeman JP. Complex networks orchestrate epithelial-mesenchymal transitions. *Nat Rev Mol Cell Biol* 2006; **7**: 131–142.
4. Zavadil J, Bottinger EP. TGF-beta and epithelial-to-mesenchymal transitions. *Oncogene* 2005; **24**: 5764–5774.
5. Lamouille S, Derynck R. Cell size and invasion in TGF-beta-induced epithelial to mesenchymal transition is regulated by activation of the mTOR pathway. *J Cell Biol* 2007; **178**: 437–451.
6. Penafuerte C, Galipeau J. TGF beta secreted by B16 melanoma antagonizes cancer gene immunotherapy bystander effect. *Cancer Immunol Immunother* 2008; **57**: 1197–1206.
7. Maitra M, Cano CA, Garcia CK. Mutant surfactant A2 proteins associated with familial pulmonary fibrosis and lung cancer induce TGF-beta1 secretion. *Proc Natl Acad Sci USA* 2012; **109**: 21064–21069.
8. Curran CS, Keely PJ. Breast tumor and stromal cell responses to TGF-beta and hypoxia in matrix deposition. *Matrix Biol* 2012; **32**: 95–105.
9. Roberts AB, McCune BK, Sporn MB. TGF-beta: regulation of extracellular matrix. *Kidney Int* 1992; **41**: 557–559.
10. Kumawat K, Menzen MH, Bos IS, Baarsma HA, Borger P, Roth M *et al.* Noncanonical WNT-5 A signaling regulates TGF-beta-induced extracellular matrix production by airway smooth muscle cells. *FASEB J* 2012; **27**: 1631–1643.
11. Goc A, Choudhary M, Byzova TV, Somanath PR. TGFbeta- and bleomycin-induced extracellular matrix synthesis is mediated through Akt and mammalian target of rapamycin (mTOR). *J Cell Physiol* 2011; **226**: 3004–3013.
12. Siegel PM, Massague J. Cytostatic and apoptotic actions of TGF-beta in homeostasis and cancer. *Nat Rev Cancer* 2003; **3**: 807–821.
13. Tang B, Vu M, Booker T, Santner SJ, Miller FR, Anver MR *et al.* TGF-beta switches from tumor suppressor to prometastatic factor in a model of breast cancer progression. *J Clin Invest* 2003; **112**: 1116–1124.
14. Derynck R, Akhurst RJ, Balmain A. TGF-beta signaling in tumor suppression and cancer progression. *Nat Genet* 2001; **29**: 117–129.
15. Kang Y, Massague J. Epithelial-mesenchymal transitions: twist in development and metastasis. *Cell* 2004; **118**: 277–279.
16. Peinado H, Olmeda D, Cano A. Snail, Zeb and bHLH factors in tumour progression: an alliance against the epithelial phenotype? *Nat Rev Cancer* 2007; **7**: 415–428.
17. Van Themsche C, Chaudhry P, Leblanc V, Parent S, Asselin E. XIAP gene expression and function is regulated by autocrine and paracrine TGF-beta signaling. *Mol Cancer* 2010; **9**: 216.
18. Shi Y, Massague J. Mechanisms of TGF-beta signaling from cell membrane to the nucleus. *Cell* 2003; **113**: 685–700.
19. Derynck R, Zhang YE. Smad-dependent and Smad-independent pathways in TGF-beta family signalling. *Nature* 2003; **425**: 577–584.
20. Singh M, Chaudhry P, Parent S, Asselin E. Ubiquitin-proteasomal degradation of COX-2 in TGF-beta stimulated human endometrial cells is mediated through endoplasmic reticulum mannosidase I. *Endocrinology* 2012; **153**: 426–437.
21. El-Guendy N, Zhao Y, Gurumurthy S, Burikhanov R, Rangnekar VM. Identification of a unique core domain of par-4 sufficient for selective apoptosis induction in cancer cells. *Mol Cell Biol* 2003; **23**: 5516–5525.
22. Zapata-Benavides P, Mendez-Vazquez JL, Gonzalez-Rocha TR, Zamora-Avila DE, Franco-Molina MA, Garza-Garza R *et al.* Expression of prostate apoptosis response (Par-4) is associated with progesterone receptor in breast cancer. *Arch Med Res* 2009; **40**: 595–599.
23. Moreno-Bueno G, Fernandez-Marcos PJ, Collado M, Tendero MJ, Rodriguez-Pinilla SM, Garcia-Cao I *et al.* Inactivation of the candidate tumor suppressor par-4 in endometrial cancer. *Cancer Res* 2007; **67**: 1927–1934.
24. Cook J, Krishnan S, Ananth S, Sells SF, Shi Y, Walther MM *et al.* Decreased expression of the pro-apoptotic protein Par-4 in renal cell carcinoma. *Oncogene* 1999; **18**: 1205–1208.
25. Nalca A, Qiu SG, El-Guendy N, Krishnan S, Rangnekar VM. Oncogenic Ras sensitizes cells to apoptosis by Par-4. *J Biol Chem* 1999; **274**: 29976–29983.
26. Zhao Y, Rangnekar VM. Apoptosis and tumor resistance conferred by Par-4. *Cancer Biol Ther* 2008; **7**: 1867–1874.
27. Van Themsche C, Mathieu I, Parent S, Asselin E. Transforming growth factor-beta3 increases the invasiveness of endometrial carcinoma cells through phosphatidylinositol 3-kinase-dependent up-regulation of X-linked inhibitor of apoptosis and protein kinase c-dependent induction of matrix metalloproteinase-9. *J Biol Chem* 2007; **282**: 4794–4802.
28. Zeinoun Z, Teugels E, De Bleser PJ, Neyns B, Geerts A, De Greve J. Insufficient TGF-beta 1 production inactivates the autocrine growth suppressive circuit in human ovarian cancer cell lines. *Anticancer Res* 1999; **19**: 413–420.
29. Yang L, Yang J, Venkateswarlu S, Ko T, Brattain MG. Autocrine TGFbeta signaling mediates vitamin D3 analog-induced growth inhibition in breast cells. *J Cell Physiol* 2001; **188**: 383–393.
30. Inman GJ, Nicolas FJ, Callahan JF, Harling JD, Gaster LM, Reith AD *et al.* SB-431542 is a potent and specific inhibitor of transforming growth factor-beta superfamily type I activin receptor-like kinase (ALK) receptors ALK4, ALK5, and ALK7. *Mol Pharmacol* 2002; **62**: 65–74.
31. Saegusa M, Hashimura M, Kuwata T, Okayasu I. Transcriptional regulation of pro-apoptotic Par-4 by NF-kappaB/p65 and its function in controlling cell kinetics during early events in endometrial tumourigenesis. *J Pathol* 2010; **221**: 26–36.
32. Lei X, Wang L, Yang J, Sun LZ. TGFbeta signaling supports survival and metastasis of endometrial cancer cells. *Cancer Manag Res* 2009; **2009**: 15–24.
33. Szasz AM, Tokes AM, Micsinai M, Krenacs T, Jakab C, Lukacs L *et al.* Prognostic significance of claudin expression changes in breast cancer with regional lymph node metastasis. *Clin Exp Metastasis* 2011; **28**: 55–63.
34. Myal Y, Leygue E, Blanchard AA. Claudin 1 in breast tumorigenesis: revelation of a possible novel 'claudin high' subset of breast cancers. *J Biomed Biotechnol* 2010; **2010**: 956897.
35. Swisshelm K, Macek R, Kubbies M. Role of claudins in tumorigenesis. *Adv Drug deliv Rev* 2005; **57**: 919–928.
36. Tokes AM, Kulka J, Paku S, Szik A, Paska C, Novak PK *et al.* Claudin-1, -3 and -4 proteins and mRNA expression in benign and malignant breast lesions: a research study. *Breast Cancer Res* 2005; **7**: R296–R305.
37. Chaudhry P, Singh M, Parent S, Asselin E. Prostate apoptosis response 4 (Par-4), a novel substrate of caspase-3 during apoptosis activation. *Mol Cell Biol* 2012; **32**: 826–839.
38. Koinuma D, Tsutsumi S, Kamimura N, Imamura T, Aburatani H, Miyazono K. Promoter-wide analysis of Smad4 binding sites in human epithelial cells. *Cancer Sci* 2009; **100**: 2133–2142.
39. Zawel L, Dai JL, Buckhaults P, Zhou S, Kinzler KW, Vogelstein B *et al.* Human Smad3 and Smad4 are sequence-specific transcription activators. *Mol Cell* 1998; **1**: 611–617.
40. Dennler S, Itoh S, Vivien D, ten Dijke P, Huet S, Gauthier JM. Direct binding of Smad3 and Smad4 to critical TGF beta-inducible elements in the promoter of human plasminogen activator inhibitor-type 1 gene. *EMBO J* 1998; **17**: 3091–3100.
41. Kim J, Johnson K, Chen HJ, Carroll S, Laughon A. Drosophila Mad binds to DNA and directly mediates activation of vestigial by Decapentaplegic. *Nature* 1997; **388**: 304–308.
42. Labbe E, Silvestri C, Hoodless PA, Wrana JL, Attisano L. Smad2 and Smad3 positively and negatively regulate TGF beta-dependent transcription through the forkhead DNA-binding protein FAST2. *Mol Cell* 1998; **2**: 109–120.
43. Massague J, Seoane J, Wotton D. Smad transcription factors. *Genes Dev* 2005; **19**: 2783–2810.
44. Garcia-Cao I, Lafuente MJ, Criado LM, Diaz-Meco MT, Serrano M, Moscat J. Genetic inactivation of Par4 results in hyperactivation of NF-kappaB and impairment of JNK and p38. *EMBO Rep* 2003; **4**: 307–312.
45. Martinez-Estrada OM, Lettice LA, Essafi A, Guadix JA, Slight J, Velecela V *et al.* Wt1 is required for cardiovascular progenitor cell formation through transcriptional control of Snail and E-cadherin. *Nat Genet* 2010; **42**: 89–93.
46. Dhasarathy A, Phadke D, Mav D, Shah RR, Wade PA. The transcription factors Snail and Slug activate the transforming growth factor-beta signaling pathway in breast cancer. *PLoS ONE* 2011; **6**: e26514.
47. Dhasarathy A, Kajita M, Wade PA. The transcription factor snail mediates epithelial to mesenchymal transitions by repression of estrogen receptor-alpha. *Mol Endocrinol* 2007; **21**: 2907–2918.
48. Prat A, Parker JS, Karginova O, Fan C, Livasy C, Herschkowitz JI *et al.* Phenotypic and molecular characterization of the claudin-low intrinsic subtype of breast cancer. *Breast Cancer Res* 2010; **12**: R68.
49. Chapdelaine P, Kang J, Boucher-Kovalik S, Caron N, Tremblay JP, Fortier MA. Decidualization and maintenance of a functional prostaglandin system in human endometrial cell lines following transformation with SV40 large T antigen. *Mol Hum Reprod* 2006; **12**: 309–319.

Supplementary Information accompanies this paper on Cell Death and Disease website (http://www.nature.com/cddis)